

Published in final edited form as:

Exp Eye Res. 2011 December ; 93(6): 912–920. doi:10.1016/j.exer.2011.10.007.

Spatial analysis of human lens aquaporin-0 post-translational modifications by MALDI mass spectrometry tissue profiling

Danielle B. Gutierrez¹, Donita Garland², and Kevin L. Schey³

¹Laboratory of Retinal Cell Molecular Biology, National Eye Institute, National Institutes of Health

²Department of Ophthalmology, University of Pennsylvania

³Mass Spectrometry Research Center and Department of Biochemistry, Vanderbilt University School of Medicine

Abstract

Aquaporin 0 (AQP0), the major integral membrane protein in lens fiber cells, becomes highly modified with increasing age. The functional consequences of these modifications are being revealed, and the next step is to determine how these modifications affect the ocular lens, which is directly related to their abundances and spatial distributions. The aim of this study was to utilize matrix-assisted laser desorption ionization (MALDI) direct tissue profiling methods, which produce spatially-resolved protein profiles, to map and quantify AQP0 post-translational modifications (PTMs). Direct tissue profiling was performed using frozen, equatorial human lens sections of various ages prepared by conditions optimized for MALDI mass spectrometry profiling of membrane proteins. Modified forms of AQP0 were identified and further investigated using liquid chromatography tandem mass spectrometry (LC-MS/MS). The distributions of unmodified, truncated, and oleoylated forms of AQP0 were examined with a maximum spatial resolution of 500 μm . Direct tissue profiling of intact human lens sections provided high quality, spatially-resolved, relative quantitative information of AQP0 and its modified forms indicating that 50% of AQP0 is truncated at a fiber cell age of 24 \pm 1 year in all lenses examined. Furthermore, direct tissue profiling also revealed previously unidentified AQP0 modifications including N-terminal acetylation and carbamylation. N-terminal acetylation appears to provide a protective effect against N-terminal truncation.

Keywords

MALDI tissue profiling; membrane proteins; aquaporin; protein modification

Introduction

In the ocular lens, lifelong differentiation of epithelial cells into fiber cells produces concentric layers of fibers, with the oldest fiber cells in the lens center/core and the newest, youngest fiber cells in the lens periphery/cortex (Kuszak, 1995; Mathias et al., 1997, 2007).

© 2011 Elsevier Ltd. All rights reserved.

Corresponding Author: Kevin L. Schey, Mass Spectrometry Research Center, Vanderbilt University, 465 21st Ave. So., Suite 9160 MRB III, Phone: 615-936-6861, Kevin.schey@vanderbilt.edu.

Publisher's Disclaimer: This is a PDF file of an unedited manuscript that has been accepted for publication. As a service to our customers we are providing this early version of the manuscript. The manuscript will undergo copyediting, typesetting, and review of the resulting proof before it is published in its final citable form. Please note that during the production process errors may be discovered which could affect the content, and all legal disclaimers that apply to the journal pertain.

Thus, the ocular lens is a model tissue for studying age related protein modifications (Kuszak, 1995; Mathias et al., 1997, 2007; Ball et al., 2004). The major integral membrane protein in lens fiber cells is aquaporin 0 (AQP0), which composes greater than 50% of the membrane protein content (Broekhuysen et al., 1976; Varadaraj et al., 1999; Ball et al., 2004) and is known to be modified with age (Takemoto et al., 1986; Takemoto and Takehana, 1986).

AQP0 functions as a water transport channel (Varadaraj et al., 1999, 2005) and also serves as an adhesion protein, forming thin junctions between fiber cells (Zampighi et al., 1989; Gonen et al., 2004b; Kumari et al., 2011). Early studies were carried out on either whole lenses or lenses dissected into cortex and nucleus regions and, through Western blot analysis, determined that the C-terminus of AQP0 was truncated with age (Takemoto et al., 1986; Takemoto and Takehana, 1986). Further characterization of AQP0 in human lenses of various ages was accomplished by homogenization and digestion of the protein followed by liquid chromatography tandem mass spectrometry (LC-MS/MS) (Schey et al., 2000; Ball et al., 2004). These studies revealed specific sites of modification on the C-terminus, including abundant truncation at asparagine 246 (N246) and N259, less abundant truncations at multiple residues of the distal C-terminus, deamidation (Schey et al., 2000; Ball et al., 2004), racemization, isomerization, and phosphorylation at serine residues 229 (S229), S231, and S235 (Ball et al., 2004). While these studies provided valuable data for specific sites of modifications, the spatial resolution was limited to either the whole lens (Schey et al., 2000) or lenses dissected into 3-4 regions (Ball et al., 2004). More recently, AQP0 was characterized by Western blotting and MALDI-TOF MS (Korlimbinis et al., 2009), where the extent of C-terminal truncation was quantified in various aged lenses dissected into 4 regions (Korlimbinis et al., 2009).

The functional role of some of these modifications is emerging. AQP0 truncation increases with fiber cell and lens age (Schey et al., 2000; Ball et al., 2004; Korlimbinis et al., 2009), and it has been shown that C-terminal truncation of AQP0 leads to the formation of AQP0 junctions (Gonen et al., 2004a) and potential loss of interactions with cytoskeletal proteins (Lindsey Rose et al., 2006). Furthermore, it has been proposed that AQP0 C-terminal truncation may eventually permit obstruction of the AQP0 pore, leading to the formation of a water permeability barrier (Korlimbinis et al., 2009). Phosphorylation at S235 reduces the binding of AQP0 with Ca²⁺-calmodulin (Rose et al., 2008; Reichow and Gonen, 2008) and alters AQP0 water permeability (Kalman et al., 2008). Additionally, phosphorylation may play a role in AQP0 transport to the membrane (Golestaneh et al., 2008). Determination of the spatial distributions of these modifications is essential to understand how they affect fiber cell function in discrete lenticular locations as well as how they affect whole lens function and transparency.

Recently, a method was developed to profile membrane proteins directly from tissue, allowing for the analysis of intact AQP0 with improved spatial resolution (Thibault et al., 2008). Direct tissue profiling from intact tissue sections minimizes sample processing, reducing the potential loss of modifications (Schwartz et al., 2003) and artifactual modification of proteins, such as carbamylation which can result from urea washes (Xiang et al., 1998; Lapko et al., 2001, 2003). Thus, direct tissue profiling allows for the detection of endogenous modifications that may otherwise not be observed and allows for direct comparison of intact modified protein to unmodified protein. The advantages of this method are demonstrated by the discovery of novel PTMs to AQP0, N-linked oleoylation and palmitoylation, which were first observed by MALDI direct tissue profiling (Schey et al., 2010). This method also led to a protocol for imaging membrane proteins directly from tissue (Grey et al., 2009a). Imaging has the advantage of achieving greater spatial resolution, while profiling provides increased signal and mass resolution.

The aim of the present study was to spatially resolve PTMs of AQP0 directly from human lens tissue sections of various ages using this recently developed method for direct tissue profiling of membrane proteins (Thibault et al., 2008). This analysis revealed regions of distinct transition in AQP0 modification as a result of lens fiber cell differentiation and/or age-related changes. Both known and novel modifications were detected and mapped with a spatial resolution of 500 μm .

Methods

Materials

Lenses were obtained from NDRI (Philadelphia, PA) or as a gift from the Garland laboratory at University of Pennsylvania. HPLC grade water, acetonitrile (MeCN), and trifluoroacetic acid (TFA) were all obtained through Thermo Fisher Scientific (Suwanee, GA). Hexafluoroisopropanol (HFIP), formic acid (FA), and 3,5-dimethoxy-4-hydroxycinnamic acid matrix (sinapinic acid, SA) were obtained through Sigma Aldrich (St. Louis, MO). Tissue freezing medium was obtained from Triangle Biomedical Sciences, Inc. (Durham, NC).

Direct Tissue Profiling

Frozen human lenses of age 7, 25, 32, 43, and 69 years were sectioned as described previously (Thibault et al., 2008; Grey et al., 2009a). Equatorial lens sections were acquired at a thickness of 20 μm and a temperature of -20°C and thaw mounted onto conductive glass slides coated with a thin layer of methanol (Thibault et al., 2008; Grey et al., 2009a).

The mounted lens sections were subjected to a series of water washes to reduce the presence of soluble crystallin proteins and improve AQP0 signal. Water, $\leq 250 \mu\text{L}$, was placed on top of the thawed lens sections for 1 minute, removed, and the sections were allowed to dry for 4 minutes before the process was repeated a total of two (69 and 43 year lenses) or three times (7 year lenses). After washing, the sections were allowed to air dry completely and the cycle was repeated a second time. Alternatively, to promote section adherence to the slide and minimize tissue delocalization, some lens sections (25 and 32 yr) were washed with water for 1 minute and then placed in a dessicator until completely dried (Grey et al., 2009a). This was performed a total of six times.

To solubilize the membrane proteins, $\leq 0.1 \mu\text{L}$ of 7:3 formic acid:hexafluoroisopropanol (FA:HFIP) (Schey, 1996) was spotted onto completely dried lens sections. While the tissue was still wet, approximately $0.1 \mu\text{L}$ of matrix (saturated SA in 90% MeCN, 0.1% TFA) was applied (spotted 2-4 times as it dried) (Thibault et al., 2008). FA:HFIP and matrix were deposited in 5-6 regions from the cortex to the core of the lens.

A Bruker Autoflex III TOF mass spectrometer (Bruker Daltonics, Bremen Germany) in positive ion, linear mode was used to analyze the lens sections, as described previously (Thibault et al., 2008). Post-acquisition, the radius of each lens and the approximate radial distance of each spot (region) were determined using a scanned image of the section. As in Jacobs et al. (2004), radial distance (r) was normalized to lens radius (a) to determine normalized lens distance (r/a) and compare regions in lenses of different radii. Normalized distances of 0 and 1 represent the lens center and periphery, respectively (Jacobs et al., 2004).

To quantitate the average percent truncation across the lens regions and in lenses of various ages, the intensity of each truncated product was divided by the summed intensities of truncated and intact AQP0. Peak intensities were obtained from MALDI spectra ($n = 2-18$) acquired from each lens age and region. In some cases modified or unmodified AQP0 peaks

could not be resolved in all of the spectra. For example, in the embryonic nucleus intact AQP0 was not always resolved, precluding the relative quantitation of truncated AQP0 in this region from all collected spectra. For this reason, various numbers of spectra (2-18) were used to obtain the average percent of modification, with the exception of the embryonic nucleus from the 43 yr lens, where both intact AQP0 and AQP0 1-246 were resolved in only one spectrum.

Identification and spatial distribution of AQP0 N-terminal acetylation

Fresh eyes were obtained from the NDRI within 36 hours of removal from the donor. Human lenses of various ages were dissected into 5-7 regions based on developmental fiber cell age as described previously (Garland et al., 1996). To establish the radial position of each dissected lens region, the diameters of the intact lenses and of the undissected lens sections were measured as shells of fiber cells were removed during the dissection. Dissected fiber cell regions were stored at -80 °C until analysis (Garland et al., 1996). The dissected lens regions were shipped on dry ice overnight and stored at -80 °C. To compare dissected regions from different lenses, the midpoint distance of each shell (based on the above measured diameters) was determined and normalized as a function of the intact lens size, in a similar manner to Jacobs et al. (2004).

For identification and semi-quantitative LC-MS analysis of acetylation, lenses were processed in pairs, aged and young, in a manner similar to that previously described (Ball et al., 2004). Membrane protein pellets were suspended in 180 µL of 50 mM NH₄HCO₃, and after sonication for 2 minutes, 20 µL of MeCN was added. Trypsin (1-2 µg) was added and the samples were digested for 24 hours at 37°C. After digestion, samples were spun at 16,000 × g at 4°C for 10 minutes. Protein assays of the digested samples were carried out using the bicinchoninic acid (BCA) assay (Pierce) with digested, bovine serum albumin (BSA) as a standard.

All samples were analyzed on a Thermo Scientific LTQ XL Orbitrap mass spectrometer interfaced via a nanospray ionization source to an Eksigent nano LC 2D uPLC pump. Samples were queued in a Thermo Scientific Micro autosampler, chilled to 4°C, and 1.5 pmol of sample were injected. Peptides were loaded onto a C₁₈, 100 µm id, 6 cm trap column in 98% mobile phase A (100% H₂O, 0.1% formic acid) and 2% mobile phase B (100% MeCN, 0.1% formic acid) for 10 minutes. Peptides were separated on a 100 µm id, 20 cm C18 analytical column with a 23 minute gradient from 2-25% mobile phase B. Mass spectrometry analysis occurred in two stages – identification and quantitation. For identification, MS scans (m/z 250-1200) were performed in the Orbitrap followed by collision induced dissociation of selected ions and MSMS acquisition in the LTQ linear ion trap. For quantitation, MS scans were carried out in the LTQ XL ion trap, and ions of m/z 350-800 were detected. Triplicate samples were injected. Areas under the curve (AUC) were determined for acetylated and unmodified AQP0 1-5 from their respective selected ion chromatograms (SIC). Percent acetylation was calculated as

$$\% \text{ acetylation} = \text{AUC}_{\text{acet}} / (\text{AUC}_{\text{acet}} + \text{AUC}_{\text{unmod}}) \times 100 \quad \text{Eq. 1}$$

where AUC_{acet} is the AUC for the acetylated form of the peptide and AUC_{unmod} is the AUC for the unmodified form of the peptide. To determine the amount of acetylated or unmodified AQP0 1-5 independent of each other, the AUC for the acetylated or unmodified AQP0 N-terminal peptide was divided by the AUC for an unrelated internal peptide standard (AUC_{IS}), which was spiked into the sample after tryptic digestion. This ratio was multiplied by the absolute amount of the internal standard (AQ_{IS}) injected in each sample, to normalize the AUC for the peptides of interest in each sample to the amount of sample injected.

$$\text{Amt} = (\text{AUC}_{\text{acet}} / \text{AUS}_{\text{IS}}) \times \text{AQ}_{\text{IS}} \quad \text{Eq. 2}$$

$$\text{Amt} = (\text{AUC}_{\text{unmod}} / \text{AUC}_{\text{IS}}) \times \text{AQ}_{\text{IS}} \quad \text{Eq. 3}$$

Results

MALDI direct tissue profiling

Human lenses of age 7, 25, 32, 43, and 69 years were analyzed by MALDI direct tissue profiling and modifications to intact AQP0 were mapped from the cortex to the core of lens equatorial sections to determine changes to AQP0 with lens and fiber cell age. The average diameter for all aged lenses was 9.3 ± 0.84 mm, and lens sections were profiled with a spatial resolution of 0.5-1 mm, allowing for 5-6 regions to be profiled from the lens periphery to the lens center.

Figure 1 shows scanned images of human lens sections after washing (Figure 1A) and after matrix deposition (Figure 1B). The region profiled at each matrix spot was determined by measuring the radial distance of each spot from the lens center. To compare regions from lenses of different radii, radial distances (r) were normalized by dividing by the lens radius (a), as done previously (Jacobs et al., 2004). Normalized distances of 0 and 1 represent the lens center and the outer edge of the tissue section, respectively (Figure 1B). The regions sampled were correlated with developmental age (Taylor et al., 1996), as shown in Table 1. Different modified forms of AQP0 detected in MALDI profiles are discussed in separate sections below.

Truncation

Qualitative examination of the outer cortex region of the profiles shows a strong signal for the $[\text{M}+\text{H}]^+$ ion of intact AQP0 1-263 (expected m/z 28,123), which was observed at m/z 28,126; 28,110; and 28,123 for lenses of age 7, 32, and 69 years as shown in Figures 2A, 3A, and Supplementary Figure 1A, respectively. A list of expected masses of $[\text{M}+\text{H}]^+$ ions for profiled AQP0 truncation products is presented in Table 2. Further examination of each lens region at a specific age shows that signal intensities of AQP0 truncation products increase with fiber cell age, from the cortex of the lens to the core (Figures 2, 3, and Supplementary Figure 1), with the most abundant truncation occurring at residues N246 (expected m/z 26,359), N259 (expected m/z 27,710), and N243 (expected m/z 26,059). This is in agreement with previous studies (Schey et al., 2000; Ball et al., 2004) that indicate truncation at the C-terminal side of these asparagine residues is non-enzymatic and occurs with increasing age as a result of succinimide ring formation and spontaneous backbone cleavage (Ball et al., 2004).

To quantitate these findings, the percent of truncated AQP0 1-246 was determined as a function of lens age, as shown in Figure 4. At any particular age, the highest percent of truncated AQP0 1-246 is concentrated in the central regions of the lens (juvenile nucleus, fetal nucleus, and embryonic nucleus), with very little truncated product in the cortex. This is in agreement with a recent MALDI imaging study (Grey et al., 2009a). These data also show that within a particular region, truncation increases slowly with increasing lens age. For example, in the embryonic nucleus of a 7 year lens truncated AQP0 1-246 constitutes approximately 40% of total AQP0, which increases to 50% by 25 years of age and nearly 80% by 70 years of age. Note that the change in slope at approximately 30 years could be

due to a change in lens environment increasing the susceptibility of AQP0 to truncation, perhaps due to a structural change.

The percent of truncated AQP0 was also plotted as a function of normalized lens distance, as shown in Figure 5 for two major truncation sites, AQP0 1-259 (Figure 5A) and AQP0 1-246 (Figure 5B). These curves show that in 7, 25, 32, and 43 year lenses truncation increases steadily from a normalized lens distance of 1 to approximately 0.5, at which point the increase in truncation plateaus in the older lenses. In the 69 year lens, truncation increases most rapidly from a normalized lens distance of 1 to approximately 0.8 (see also Supplementary Figure 1) most likely due to the steeper age gradient in older lenses.

In order to estimate the amount of time it takes for 50% of AQP0 to become truncated to AQP0 1-246, it is necessary to know the radial distance at which this amount of truncation occurs and the age of the fiber cells at this radial distance. Since the percent of AQP0 truncation was determined as a function of radial distance (Figure 5), fiber cell age was estimated using the following equation,

$$\text{Fiber cell age} = (1/r/a) / (0.52/\text{lens age}) \quad \text{Eq. 4}$$

where r/a = the normalized lens distance and 0.52 is the normalized distance remaining from the lens periphery in an adult lens ($r/a = 1$) to the embryonic nucleus ($r/a = 0.48$). These values are based on measurements by Taylor et al. (1996) and the linear rate of lens growth from ages 10-60 (Sakabe et al., 1998; Schachar, 2005). Figure 5B shows that the amount of AQP0 1-246 reaches 50% at normalized lens distances of 0.82, 0.73, and 0.62 in 69, 43, and 32 year lenses, respectively. Using the equation above, these radial distances represent fiber cells that are approximately 24, 22, and 23 years of age, in 69, 43, and 32 year lenses, respectively. Additionally, Figure 4 shows that the amount of AQP0 1-246 reaches 50% in the embryonic nucleus ($r/a = 0$) of a 25 year lens, in agreement with the number of years determined for 50% AQP0 truncation in the inner core of manually dissected, homogenized lenses (Korlimbinis et al., 2009). This suggests that truncation of AQP0 to AQP0 1-246 reaches 50% in 24 ± 1 years. The direct tissue profiling data show that most of this truncation is occurring prior to a normalized lens distance of 0.5, after which point, the rate of truncation slows.

Oleoylation

Recently, a novel fatty acyl modification, N-linked oleoylation (+ 264 Da), was discovered on AQP0 at the N-terminal Met and Lys238 residues (Schey et al., 2010). This modification was first observed by MALDI direct tissue profiling as a shoulder on the AQP0 peak and subsequently identified by LC-MS/MS. MALDI direct tissue profiling and imaging revealed that this modification is most abundant in the inner cortical region of human lenses, of 11 and 29 years (Schey et al., 2010). In the present study, oleoylated AQP0 was mapped in lenses 7 to 69 years of age. A qualitative assessment of the data, suggested that this acylated form of AQP0 was absent from the cortex and became apparent around a normalized lens distance of 0.8 in all aged lenses (diamond labeled peaks in Figures 2, 3, and Supplementary Figure 1). Determination of percent oleoylation on intact AQP0 (1-263) from profiles of 11 and 32 year lenses, revealed that oleoylated AQP0 was most abundant at a radial lens distance of 0.6, or the inner edge of the adult nucleus, where it reached 50% of the total amount of AQP0 (Supplementary Figure 2). Although percent oleoylation was not determined for truncated AQP0, the profiling results show that it is also oleoylated in a similar ratio to intact AQP0 (Figures 2, 3, and Supplementary Figure 1).

Acetylation and Carbamylation

The AQP0 signals observed by MALDI profiling of lens tissue also revealed a mass shift of approximately 42 Da that became more apparent with increasing lens and fiber cell age (star labeled peaks in Figures 2, 3, and Supplemental Figure 1). Due to the mass resolution limitations in the MALDI profiling instrumentation, it is difficult to determine an exact mass shift from these data and to quantitate the extent of acetylation; therefore, LC-MS/MS of digested lens membrane preparations was used to determine accurate masses and to determine the extent of acetylation with lens fiber cell age. Distinct, reproducible retention times of two modified AQP0 peptides were observed, revealing that the N-terminal methionine of AQP0 is carbamylated, with a mass shift of 43 Da (data not shown), and acetylated, with a mass shift of 42 Da (Figure 6). In vivo carbamylation has been reported for lens proteins (Lapko et al., 2001, 2003), but carbamylation of proteins can also occur during urea washing (Xiang et al., 1998; Lapko et al., 2001, 2003). Typically, lens membrane proteins are prepared with urea washes to remove extrinsic membrane proteins. In the present study, carbamylation at the AQP0 N-terminus was detected in the core region of a 47 year lens prepared without urea washing (data not shown), suggesting that carbamylation occurs endogenously.

To investigate the distribution of acetylated AQP0, manually dissected lens regions from various aged lenses were analyzed by LC-MS. Relative quantitation indicated that the percent of acetylation increased with fiber cell and lens age, and that after a normalized lens distance of 0.85, the percent of acetylation increased rapidly in older lenses compared to younger lenses (Figure 7A). To determine if this increase was due to truncation of the AQP0 N-terminus with age (Schey et al., 2000), the relative amounts of unmodified and acetylated AQP0 N-terminal peptides were determined and plotted as a function of normalized lens distance (Figure 7B). It is evident that signal for the unmodified AQP0 N-terminus decreases rapidly at a normalized lens distance of 0.85 in the older lenses, while the relative amount of acetylated N-terminal peptide decreases at a slower rate. This suggests that the increase in percent acetylation is due to truncation of the unmodified N-terminus, that N-terminal truncation increases more rapidly in older lenses compared to younger lenses, and that acetylation of the N-terminus might slow its truncation.

Discussion

AQP0, the major integral membrane protein of the lens fiber cells, is a highly modified protein. PTMs to this protein include truncation, deamidation, isomerization, racemization, and phosphorylation (Ball et al., 2004). Many of these modifications were determined by digestion of membrane proteins prepared from whole lens homogenates or manually dissected lenses (Schey et al., 2000; Ball et al., 2004). This approach allows for sequence analysis of the peptide mixture, measurement of the exact mass shift of the modified peptides, and determination of the specific sites of modification. In this way, all of the known specific sites of modification have been located on the C-terminus of AQP0. As the major sites of AQP0 modification have been identified, determining their distributions throughout the lens is important, since their regional presence may indicate functional relevance in differentiation or aging.

In this study, a recently developed direct tissue profiling method designed for membrane protein analysis (Thibault et al., 2008) has been used to spatially resolve AQP0 modifications. MALDI tissue profiling facilitates analysis of the intact protein directly from tissue, preventing the loss of modifications due to sample enrichment and chromatographic separation (Schwartz et al., 2003), and it has provided relative quantitative information regarding endogenous modifications to AQP0. Our assumption is that the relative amounts of intact and modified AQP0 extracted from the tissue are the same across the tissue; not

that the extraction is complete. If this assumption holds, then the relative quantitation method presented is valid. Our results are in agreement with previous gel analyses of AQP0 truncation and previous LC/MS analyses of digested AQP0; therefore, we are confident in the observed changes in AQP0 modification measured by direct tissue analysis. Furthermore, the spatial localization of AQP0 within the lens measured by direct tissue profiling can be used to correlate findings with regions of physiological interest, such as organelle loss (Jacobs et al., 2004) or the lens permeability barrier, which is 6-8 mm in diameter (Korlimbinis et al., 2009). The distance of barrier formation has been equated to the interface of the cortex and nucleus (Sweeney and Truscott, 1998; Moffat et al., 1999). Using an average human lens diameter of 9 mm (Garland et al., 1996), barrier formation occurs at a normalized lens distance of 0.78 (7 mm/9 mm), within the adult nucleus region.

Truncation

The C-terminus of AQP0 is the site of protein-protein interactions and mediates AQP0 function both as an adhesion protein and as a water channel (Gonen et al., 2004b; Varadaraj et al., 2005; Lindsey Rose et al., 2006; Rose et al., 2008; Reichow and Gonen, 2008). AQP0 interacts with filensin and CP49 via its C-terminus, and it has been proposed that these interactions maintain hexagonal fiber cell shape (Lindsey Rose et al., 2006). Additionally in the rat lens, it has been suggested that AQP0-filensin interaction leads to the redistribution of AQP0 into aggregates on the broad side of fiber cells in the region just before nuclei degradation (Grey et al., 2009b). The C-terminus also modulates fiber cell adhesion, as its truncation leads to junction formation between AQP0 tetramers, strengthening fiber-to-fiber adhesion (Gonen et al., 2004b). Lastly, AQP0 C-terminal truncation may contribute to the water permeability barrier that is observed in middle aged human lenses. It has been suggested that 50% truncation of AQP0 may allow adequate levels of insoluble components/protein complexes to bind to AQP0 and block the pore, creating a water permeability barrier (Korlimbinis et al., 2009). These examples highlight the importance of the AQP0 C-terminus, and illustrate how its truncation may alter protein-protein interactions (Lindsey Rose et al., 2006) and protein function – a mechanism that has been demonstrated for pH regulation of connexin 50 (Lin et al., 1998) – especially in older fibers where protein turnover does not occur (Grey et al., 2009b).

Truncated AQP0 has been extensively examined by a variety of methods ranging from gel electrophoresis to LC-MS/MS to MALDI analysis of extracted protein (Takemoto et al., 1986; Takemoto and Takehana, 1986; Schey et al., 2000; Ball et al., 2004; Korlimbinis et al., 2009). The present work provides relative quantitation of distinct C-terminal truncation products, AQP0 1-246 and 1-259, measured directly from the tissue and correlated with lens and fiber cell age (Figure 4, Figure 5).

As expected, truncation was minimal in the cortical region (Takemoto and Takehana, 1986; Schey et al., 2000; Ball et al., 2004), at less than 10% for both AQP0 1-246 and 1-259. Previous studies have observed truncation in lenses as young as seven years (Schey et al., 2000; Korlimbinis et al., 2009). The present results show that at age seven, approximately 35% of AQP0 is truncated to AQP0 1-246 in the embryonic nucleus (Figure 2E, Figure 4, Figure 5). This corroborates a study of membrane-enriched lens homogenates that showed one-third of AQP0 was truncated by age five in the inner core (Korlimbinis et al., 2009).

In middle aged lenses a permeability barrier is observed (Sweeney and Truscott, 1998; Moffat et al., 1999; Korlimbinis et al., 2009) at a distance equivalent to a normalized lens distance of 0.78. Western blotting and densitometry analysis of intact and truncated AQP0 from manually dissected, homogenized lenses showed that 50% of AQP0 was truncated in the barrier region by approximately 47 years (Korlimbinis et al., 2009). The direct tissue profiling data support these findings, showing that 50% of AQP0 is truncated to AQP0

1-246 at a normalized lens distance of approximately 0.8 for a lens age of 55 years (Figure 4).

The high spatial resolution achieved by direct tissue profiling facilitated determination of the rate of AQP0 truncation, by correlating radial distance with estimated fiber cell age. The data suggest that 50% of AQP0 is truncated to AQP0 1-246 in 24 ± 1 years and that most of this truncation is occurring prior to a normalized lens distance of 0.5, after which point the rate of truncation slows. This slow rate of truncation supports a non-enzymatic mechanism, as truncation at asparagine residues and previous data suggest (Ball et al., 2004). In contrast, an enzymatic process would occur faster, and may be localized to a small region. For example, rat AQP0 undergoes rapid truncation over a short distance in the lens core (Thibault et al., 2008; Grey et al., 2009b) that is thought to be achieved, at least in part, by calpain (Schey et al., 1999; Grey et al., 2009b).

Oleoylation

Analysis of intact AQP0 from tissue revealed the distribution of oleoylated AQP0, which appears suddenly at a normalized lens distance of approximately 0.9-0.8 (Figure 2, Figure 3, Supplementary Figure 1) and reaches nearly 50% of the level of unmodified AQP0 at a normalized lens distance of 0.6 (Supplemental Figure 2). Oleoylated AQP0 partitions to the detergent-resistant membranes, while unmodified AQP0 is found in both detergent-soluble and detergent resistant membranes (Schey et al., 2010). The targeting of oleoylated AQP0 to detergent-resistant membranes specifically in the nuclear regions of all lenses examined suggests a significant role in regulating lens function, perhaps through organizing fiber cell membrane domains. Interestingly, fetal lenses do not contain oleoylated AQP0 (Korlimbinis et al., 2009). The exact effect of oleoylated AQP0 in this region remains to be determined, but it could alter protein-protein interactions of the AQP0 C-terminus with calmodulin and/or filensin, subsequently effecting the regulation of lens water permeability and/or fiber-fiber adhesion (Schey et al., 2010).

Acetylation and Carbamylation

Previously unreported modifications to AQP0 were detected, which have been identified as carbamylation, and acetylation at the N-terminus. The modified peptides were not initially observed by the conventional shotgun proteomics techniques of digestion and analysis of the soluble peptides. This finding demonstrates the importance of direct tissue profiling for the detection of novel modifications.

Based on MALDI profiling results, subsequent LC-MS/MS analysis allowed identification of carbamylation (data not shown) and acetylation (Figure 6) on the N-terminus of AQP0. The distribution and relative quantitation of AQP0 N-terminal acetylation were determined for various aged lenses by LC-MS analysis of manually dissected lens regions. These data revealed that the relative extent of acetylation increases with fiber cell and lens age (Figure 7). Furthermore, at normalized lens distances of less than 0.85 the signal for the unmodified N-terminal peptide rapidly decreases in the nucleus of older lenses, while the signal for the acetylated peptide decreases more gradually (Figure 7). This suggests that acetylation of the N-terminus may protect it from age-related truncation. The effect of N-terminal acetylation on AQP0 function and/or its protein-protein/protein-membrane interactions remains to be determined.

N-terminal acetylation is a common protein modification (Polevoda and Sherman, 2000, 2002) that occurs co-translationally to confer resistance to degradative processes in the cell. Although many lens proteins are acetylated, no alternative functions have been demonstrated. It has been suggested that N-terminal acetylation of connexins may have a

regulatory function (Shearer et al., 2008), since the N-terminus of connexins are important to channel permeability and gating.

The timing of acetylation (co- or post-translational) of the AQP0 N-terminus is intriguing. Presumably, co-translational acetylation would modify the entire pool of protein; since this is not the case, acetylation is likely a post-translational event (Shearer et al., 2008), occurring substoichiometrically and presumably prior to the loss of nuclei and organelles. For human AQP0, the increase in percent acetylation after the nuclei and organelles degrade is attributed to the loss of the unmodified N-terminus. Post-translational N-terminal acetylation has been detected on some hormones (Polevoda and Sherman, 2002), for example, on α -melanocyte-stimulating hormone, where acetylation increases its activity (O'Donohye et al., 1982; Polevoda and Sherman, 2002). N-terminal acetylation is also a PTM of β -endorphin, for which it reduces the activity (Smyth et al., 1979; O'Donohye et al., 1982; Polevoda and Sherman, 2002).

The distribution of carbamylated AQP0 was not determined from the direct tissue profiling data because it cannot be resolved from acetylated AQP0. Furthermore, the distribution of AQP0 carbamylation was not mapped via LC-MS/MS analysis of manually dissected lenses, as the lenses were washed with urea that can cause artifactual carbamylation. Carbamylation as a PTM has precedence in the lens, where γ B-, γ C-, and γ D-crystallins are carbamylated at their N-termini (Lapko et al., 2003), and in vivo carbamylation in the lens has been correlated with cataractogenesis (Beswick and Harding, 1984). Carbamylation can occur non-enzymatically (Beswick and Harding, 1984) and irreversibly (Beswick and Harding, 1984; Van Driessche et al., 2002), so that it is possible for this modification to increase in the lens core. At physiological pH, carbamylation (Lapko et al., 2001; Van Driessche et al., 2002) and acetylation (Lapko et al., 2001) of lysine remove the charge on this residue, leaving it as neutral, and potentially modifying protein-protein interactions (Beswick and Harding, 1984; Lapko et al., 2001). It is possible that these modifications to AQP0 alter protein-protein interactions involving its N-terminus. However, since these modifications are found in non-cataractous lenses it is unlikely that they negatively affect the function of AQP0, as suggested for N-terminal carbamylation of γ -crystallins detected in young, clear lenses (Lapko et al., 2003).

In summary, direct tissue profiling of human lenses has been used to spatially map the distribution of AQP0 and its modified forms directly from lens sections providing high quality spatial information and resolution of modifications. Direct tissue analysis led to the detection of new AQP0 modifications including carbamylation, acetylation, and oleoylation. Furthermore, the application of this technique to various aged lenses has produced a spatially-resolved semi-quantitative assessment of age-related changes in the distributions of truncated, oleoylated, and acetylated AQP0.

Supplementary Material

Refer to Web version on PubMed Central for supplementary material.

Acknowledgments

The authors acknowledge funding from NIH EY-13462 (KLS) and support from the Vanderbilt Vision Research Center (P30 EY-08126). They also acknowledge the use of the mass spectrometry facilities at Vanderbilt University and the Medical University of South Carolina.

References

- Ball LE, Garland DL, Crouch RK, Schey KL. Post-translational modifications of aquaporin 0 (AQP0) in the normal human lens: spatial and temporal occurrence. *Biochemistry*. 2004; 43:9856–9865. [PubMed: 15274640]
- Beswick HT, Harding JJ. Conformational changes induced in bovine lens alpha-crystallin by carbamylation. Relevance to cataract. *Biochem J*. 1984; 223:221–227. [PubMed: 6497840]
- Broekhuysse RM, Kuhlmann ED, Stols AL. Lens membranes II. Isolation and characterization of the main intrinsic polypeptide (MIP) of bovine lens fiber membranes. *Exp Eye Res*. 1976; 23:365–371. [PubMed: 976377]
- Garland DL, Duglas-Tabor Y, Jimenez-Asensio J, Datiles MB, Magno B. The nucleus of the human lens: demonstration of a highly characteristic protein pattern by two-dimensional electrophoresis and introduction of a new method of lens dissection. *Exp Eye Res*. 1996; 62:285–291. [PubMed: 8690038]
- Golestaneh N, Fan J, Zelenka P, Chepelinsky AB. PKC putative phosphorylation site Ser235 is required for MIP/AQP0 translocation to the plasma membrane. *Mol Vis*. 2008; 14:1006–1014. [PubMed: 18523655]
- Gonen T, Cheng Y, Kistler J, Walz T. Aquaporin-0 membrane junctions form upon proteolytic cleavage. *J Mol Biol*. 2004a; 342:1337–1345. [PubMed: 15351655]
- Gonen T, Sliz P, Kistler J, Cheng Y, Walz T. Aquaporin-0 membrane junctions reveal the structure of a closed water pore. *Nature*. 2004b; 429:193–197. [PubMed: 15141214]
- Grey AC, Chaurand P, Caprioli RM, Schey KL. MALDI imaging mass spectrometry of integral membrane proteins from ocular lens and retinal tissue. *J Proteome Res*. 2009a; 8:3278–3283. [PubMed: 19326924]
- Grey AC, Li L, Jacobs MD, Schey KL, Donaldson PJ. Differentiation-dependent modification and subcellular distribution of aquaporin-0 suggests multiple functional roles in the rat lens. *Differentiation*. 2009b; 77:70–83. [PubMed: 19281766]
- Jacobs MD, Soeller C, Sisley AMG, Cannell MB, Donaldson PJ. Gap junction processing and redistribution revealed by quantitative optical measurements of connexin46 epitopes in the lens. *Invest Ophthalmol Vis Sci*. 2004; 45:191–199. [PubMed: 14691173]
- Kalman K, Németh-Cahalan KL, Froger A, Hall JE. Phosphorylation determines the calmodulin-mediated Ca²⁺ response and water permeability of AQP0. *J Biol Chem*. 2008; 283:21278–21283. [PubMed: 18508773]
- Korlimbinis A, Berry Y, Thibault D, Schey KL, Truscott RJW. Protein aging: truncation of aquaporin 0 in human lens regions is a continuous age-dependent process. *Exp Eye Res*. 2009; 88:966–973. [PubMed: 19135052]
- Kumari SS, Eswaramoorthy S, Mathias RT, Varadaraj K. Unique and analogous functions of aquaporin 0 for fiber cell architecture and ocular lens transparency. *Biochim Biophys Acta*. 2011
- Kuszak J. The Ultrastructure of Epithelial and Fiber Cells in the Crystalline Lens. *Int Rev Cytol*. 1995; 163:305–350. [PubMed: 8522422]
- Lapko VN, Smith DL, Smith JB. In vivo carbamylation and acetylation of water-soluble human lens alphaB-crystallin lysine 92. *Protein Sci*. 2001; 10:1130–1136. [PubMed: 11369851]
- Lapko VN, Smith DL, Smith JB. Methylation and carbamylation of human gamma-crystallins. *Protein Sci*. 2003; 12:1762–1774. [PubMed: 12876325]
- Lindsey Rose KM, Gourdie RG, Prescott AR, Quinlan RA, Crouch RK, Schey KL. The C terminus of lens aquaporin 0 interacts with the cytoskeletal proteins filensin and CP49. *Invest Ophthalmol Vis Sci*. 2006; 47:1562–1570. [PubMed: 16565393]
- Lin JS, Eckert R, Kistler J, Donaldson P. Spatial differences in gap junction gating in the lens are a consequence of connexin cleavage. *Eur J Cell Biol*. 1998; 76:246–250. [PubMed: 9765054]
- Mathias RT, Rae JL, Baldo GJ. Physiological properties of the normal lens. *Physiol Rev*. 1997; 77:21–50. [PubMed: 9016299]
- Mathias RT, Kistler J, Donaldson P. The lens circulation. *J Membr Biol*. 2007; 216:1–16. [PubMed: 17568975]

- Moffat BA, Landman KA, Truscott RJ, Sweeney MH, Pope JM. Age-related changes in the kinetics of water transport in normal human lenses. *Exp Eye Res.* 1999; 69:663–669. [PubMed: 10620395]
- O'Donohy TL, Handelmann GE, Miller RL, Jacobowitz DM. N-acetylation regulates the behavioral activity of alpha-melanotropin in a multineurotransmitter neuron. *Science.* 1982; 215:1125–1127. [PubMed: 7063845]
- Polevoda B, Sherman F. Nalpha-terminal acetylation of eukaryotic proteins. *J Biol Chem.* 2000; 275:36479–36482. [PubMed: 11013267]
- Polevoda B, Sherman F. The diversity of acetylated proteins. *Genome Biol.* 2002; 3 reviews0006.
- Reichow SL, Gonen T. Noncanonical binding of calmodulin to aquaporin-0: implications for channel regulation. *Structure.* 2008; 16:1389–1398. [PubMed: 18786401]
- Rose KML, Wang Z, Magrath GN, Hazard ES, Hildebrandt JD, Schey KL. Aquaporin 0-calmodulin interaction and the effect of aquaporin 0 phosphorylation. *Biochemistry.* 2008; 47:339–347. [PubMed: 18081321]
- Sakabe I, Oshika T, Lim SJ, Apple DJ. Anterior shift of zonular insertion onto the anterior surface of human crystalline lens with age. *Ophthalmology.* 1998; 105:295–299. [PubMed: 9479290]
- Schachar RA. Growth patterns of fresh human crystalline lenses measured by in vitro photographic biometry. *J Anat.* 2005; 206:575–580. [PubMed: 15960767]
- Schey KL. Hydrophobic proteins and peptides analyzed by matrix-assisted laser desorption/ionization. *Methods Mol Biol.* 1996; 61:227–230. [PubMed: 8930876]
- Schey KL, Fowler JG, Shearer TR, David L. Modifications to rat lens major intrinsic protein in selenite-induced cataract. *Invest Ophthalmol Vis Sci.* 1999; 40:657–667. [PubMed: 10067969]
- Schey KL, Gutierrez DB, Wang Z, Wei J, Grey AC. Novel fatty acid acylation of lens integral membrane protein aquaporin-0. *Biochemistry.* 2010; 49:9858–9865. [PubMed: 20942504]
- Schey KL, Little M, Fowler JG, Crouch RK. Characterization of Human Lens Major Intrinsic Protein Structure. *Invest Ophthalmol Vis Sci.* 2000; 41:175–182. [PubMed: 10634618]
- Schwartz SA, Reyzer ML, Caprioli RM. Direct tissue analysis using matrix-assisted laser desorption/ionization mass spectrometry: practical aspects of sample preparation. *J Mass Spectrom.* 2003; 38:699–708. [PubMed: 12898649]
- Shearer D, Ens W, Standing K, Valdimarsson G. Posttranslational modifications in lens fiber connexins identified by off-line-HPLC MALDI-quadrupole time-of-flight mass spectrometry. *Invest Ophthalmol Vis Sci.* 2008; 49:1553–1562. [PubMed: 18385075]
- Smyth DG, Massey DE, Zakarian S, Finnie MD. Endorphins are stored in biologically active and inactive forms: isolation of alpha-N-acetyl peptides. *Nature.* 1979; 279:252–254. [PubMed: 440436]
- Sweeney MH, Truscott RJ. An impediment to glutathione diffusion in older normal human lenses: a possible precondition for nuclear cataract. *Exp Eye Res.* 1998; 67:587–595. [PubMed: 9878221]
- Takemoto L, Takehana M. Major intrinsic polypeptide (MIP26K) from human lens membrane: characterization of low-molecular-weight forms in the aging human lens. *Exp Eye Res.* 1986; 43:661–667. [PubMed: 3792465]
- Takemoto L, Takehana M, Horwitz J. Covalent changes in MIP26K during aging of the human lens membrane. *Invest Ophthalmol Vis Sci.* 1986; 27:443–446. [PubMed: 3949474]
- Taylor VL, al-Ghoul KJ, Lane CW, Davis VA, Kuszak JR, Costello MJ. Morphology of the normal human lens. *Invest Ophthalmol Vis Sci.* 1996; 37:1396–1410. [PubMed: 8641842]
- Thibault DB, Gillam CJ, Grey AC, Han J, Schey KL. MALDI tissue profiling of integral membrane proteins from ocular tissues. *J Am Soc Mass Spectrom.* 2008; 19:814–822. [PubMed: 18396059]
- Van Driessche G, Vandenberghe I, Jacquemotte F, Devreese B, Van Beeumen JJ. Mass spectrometric identification of in vivo carbamylation of the amino terminus of *Ectothiorhodospira mobilis* high-potential iron-sulfur protein, isozyme 1. *J Mass Spectrom.* 2002; 37:858–866. [PubMed: 12203680]
- Varadaraj K, Kushmerick C, Baldo GJ, Bassnett S, Shiels A, Mathias RT. The role of MIP in lens fiber cell membrane transport. *J Membr Biol.* 1999; 170:191–203. [PubMed: 10441663]
- Varadaraj K, Kumari S, Shiels A, Mathias RT. Regulation of aquaporin water permeability in the lens. *Invest Ophthalmol Vis Sci.* 2005; 46:1393–1402. [PubMed: 15790907]

- Xiang B, Ferretti J, Fales HM. Use of Mass Spectrometry To Ensure Purity of Recombinant Proteins: A Cautionary Note. *Anal Chem.* 1998; 70:2188–2190.
- Zampighi GA, Hall JE, Ehring GR, Simon SA. The structural organization and protein composition of lens fiber junctions. *J Cell Biol.* 1989; 108:2255–2275. [PubMed: 2738093]

Highlights

>Human AQP0 modifications were localized by direct tissue profiling mass spectrometry
>Truncated and lipidated AQP0 forms were correlated with fiber cell age >50% of AQP0 is truncated by fiber cell age of 24 years >N-terminal acetylation was discovered and seems to protect against AQP0 degradation

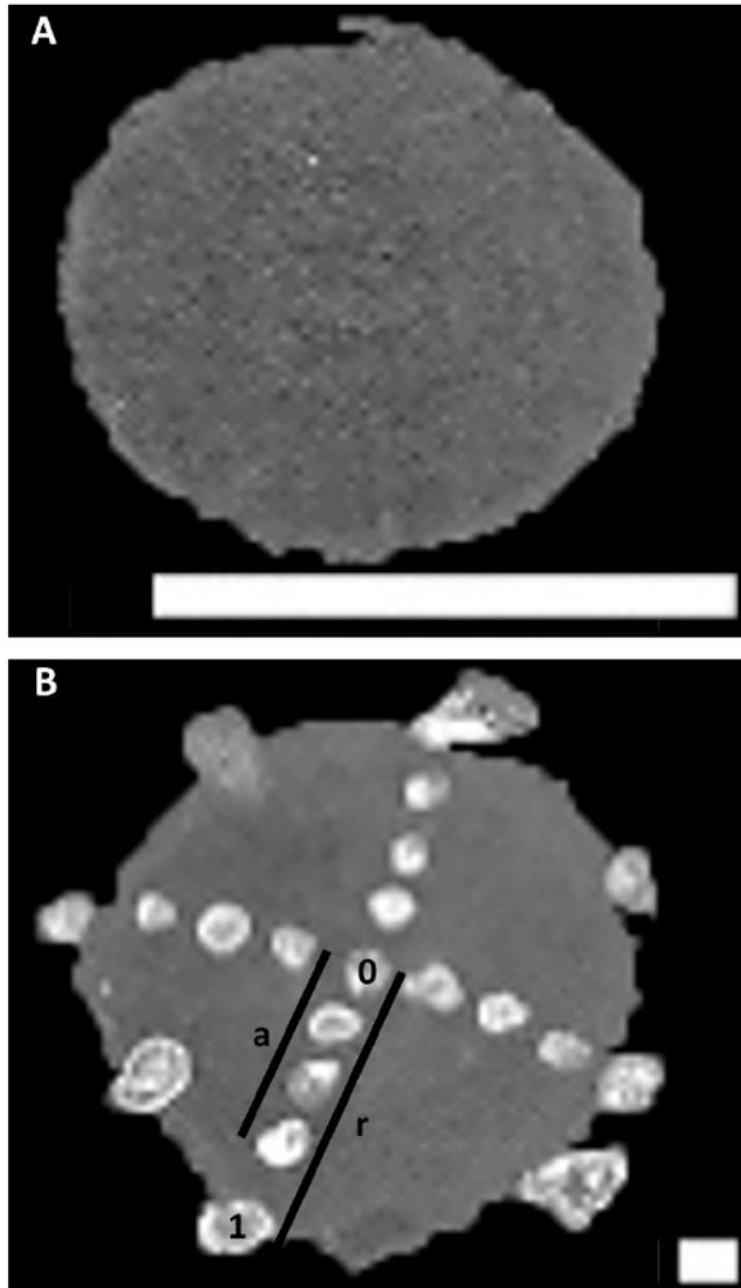


Figure 1. Scanned images of A) a 32 yr lens section after washing and B) a 25 yr lens section after washing and matrix deposition. The distance of each matrix spot from the lens center (a) was normalized to lens radius (r), yielding normalized lens distances of 0 to 1 for central to peripheral spots, respectively. The scale bars are 10 mm and 1mm in panels A and B, respectively.

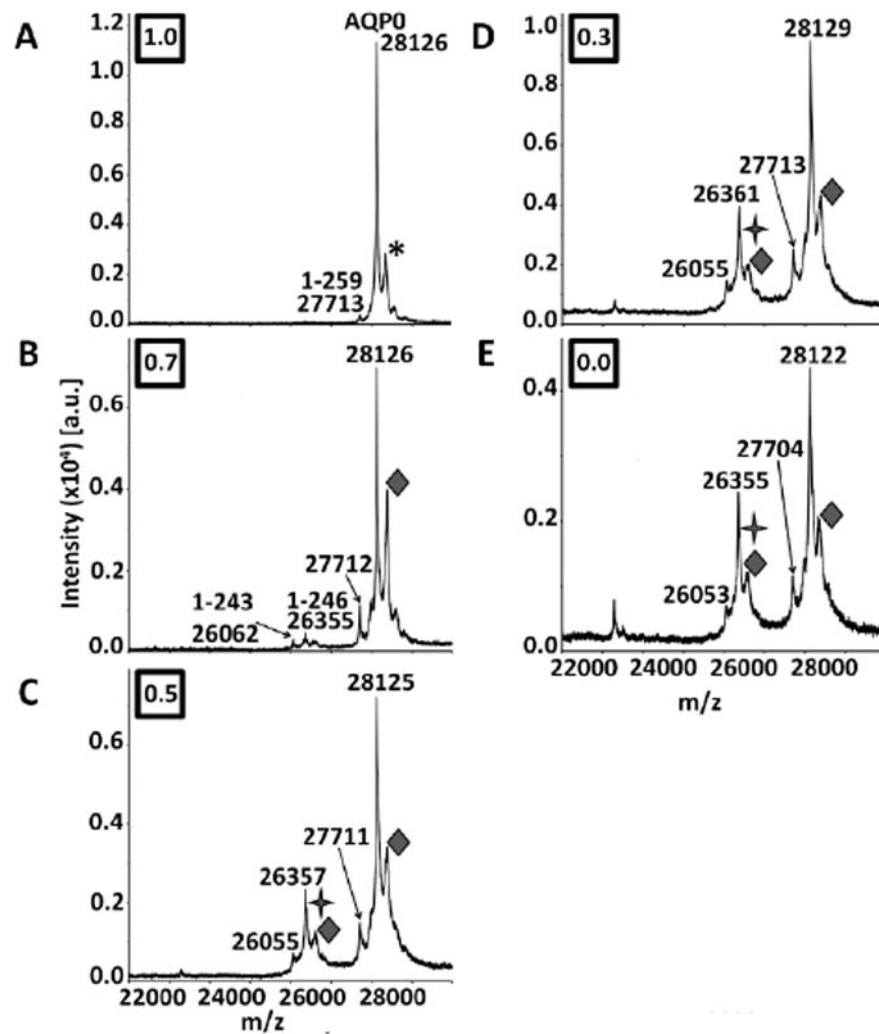


Figure 2. MALDI tissue profiles of 7 year human lens sections acquired at normalized lens distances of A) 1.0, B) 0.7, C) 0.5, D) 0.3, and E) 0.0. The diamonds (◆) indicate oleoylation of AQPO (+ 264 Da), which appears beginning at a normalized lens distance of 0.7. The stars (+) indicate acetylation (+ 42 Da), which appears as small shoulder peaks to AQPO 1-246 peaks (indicated by m/z labels) beginning at a normalized lens distance of 0.5. The AQPO label represents full length AQPO (AQPO 1-263). AQPO truncation products are represented by 1-x, where x is the C-terminal residue. The asterisk represents a sinapinic acid adduct. Boxed numbers represent the normalized lens distance from which the spectrum was obtained.

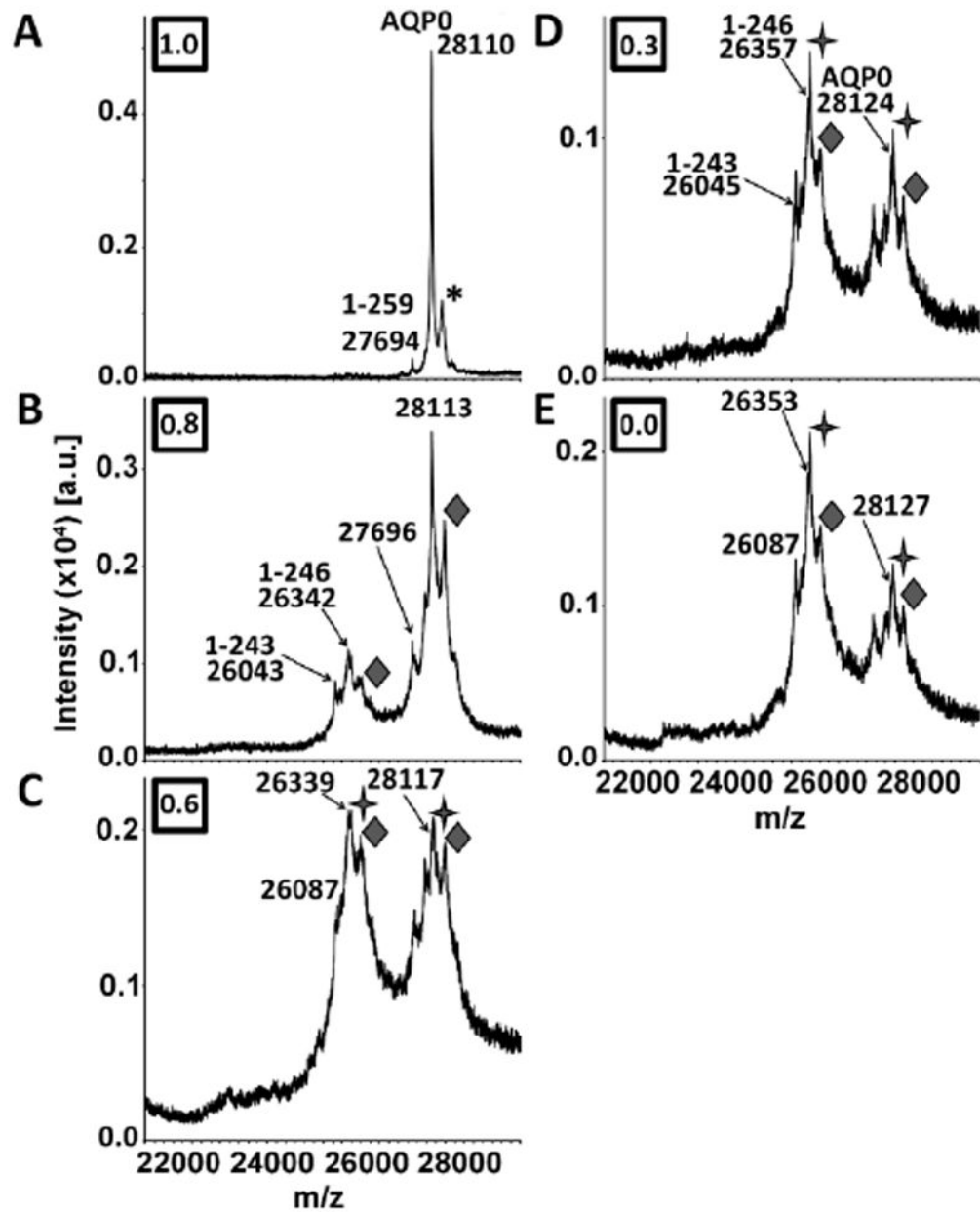


Figure 3. MALDI tissue profiles of 32 year human lens sections acquired at normalized lens distances of A) 1.0, B) 0.8, C) 0.6, D) 0.3, and E) 0.0. The diamonds (◆) indicate oleoylation of AQPO (+ 264 Da), which appears beginning at a normalized lens distance of 0.8. The stars (+) indicate acetylation (+ 42 Da), which appears as small shoulder peaks to the main truncated and intact AQPO peaks (indicated by m/z labels) beginning at a normalized lens distance of 0.6. In panels D and E, the acetylated peaks have a higher intensity than the main AQPO peaks (indicated by m/z labels). The AQPO label represents full length AQPO (AQPO 1-263). AQPO truncation products are represented by 1-x, where x is the C-terminal residue. The asterisk represents a sinapinic acid adduct. Boxed numbers represent the normalized lens distance from which the spectrum was obtained.

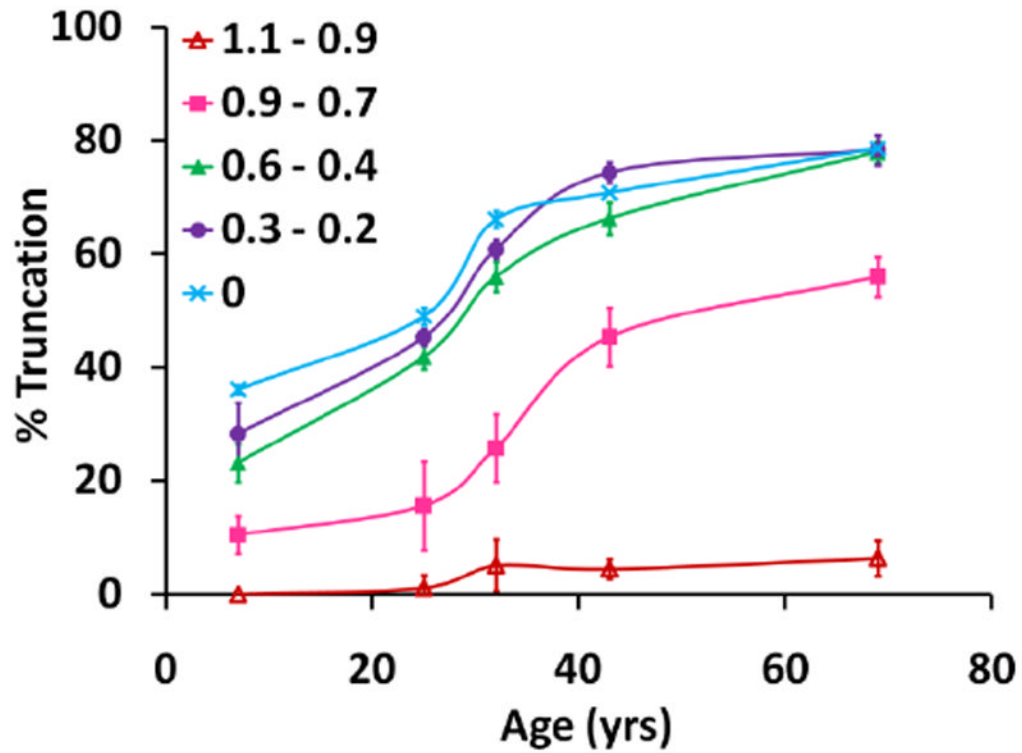


Figure 4. The distribution of truncated AQP0 1-246 as a function of lens age. For each age, the percent of truncation was determined in five regions across the lens, defined by the estimated radial distance (normalized to the lens radius) spanned by each region. The percent of truncation was calculated using the peak intensity (peak height) of truncated AQP0 compared to the total intensity for truncated AQP0 1-246 and intact AQP0.

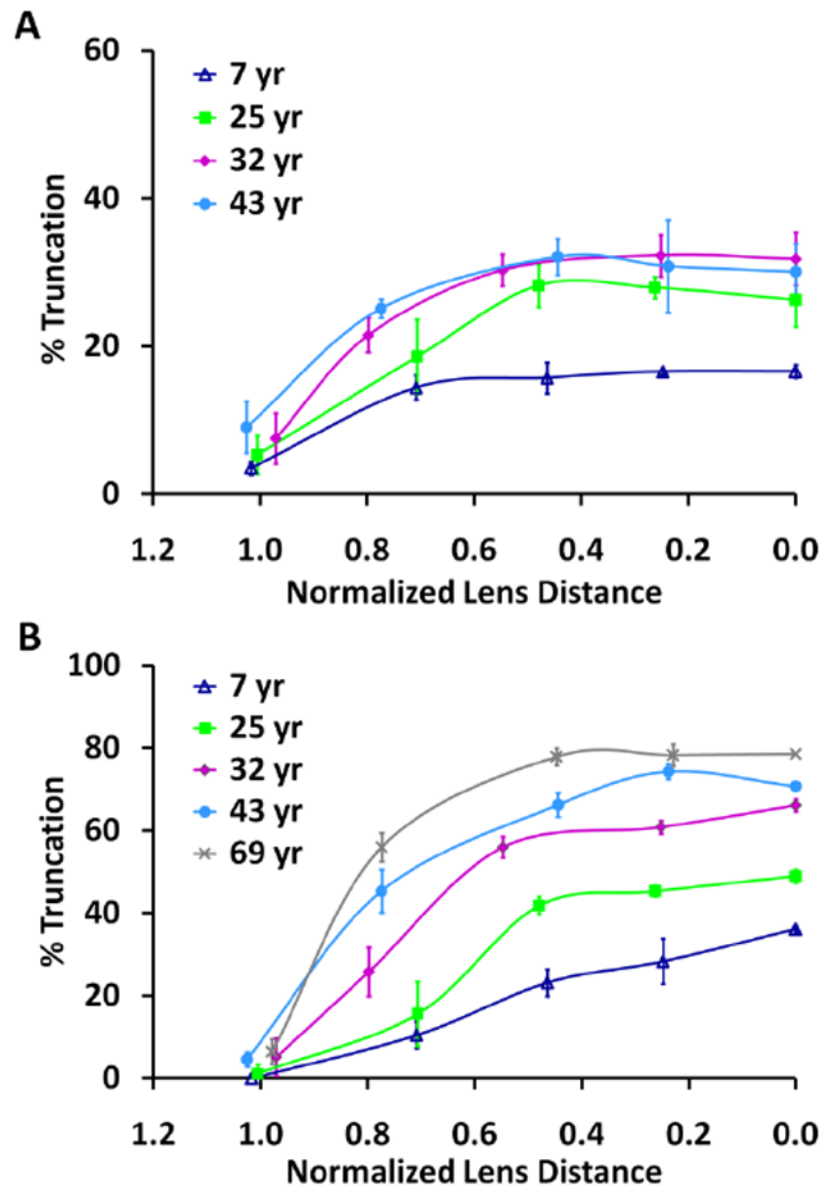


Figure 5. The distribution of truncated AQP0 as a function of normalized lens distance for A) AQP0 1-259 and B) AQP0 1-246. Truncation was calculated using the peak intensity (peak height) of truncated AQP0 compared to the total intensity of the truncated and intact AQP0.

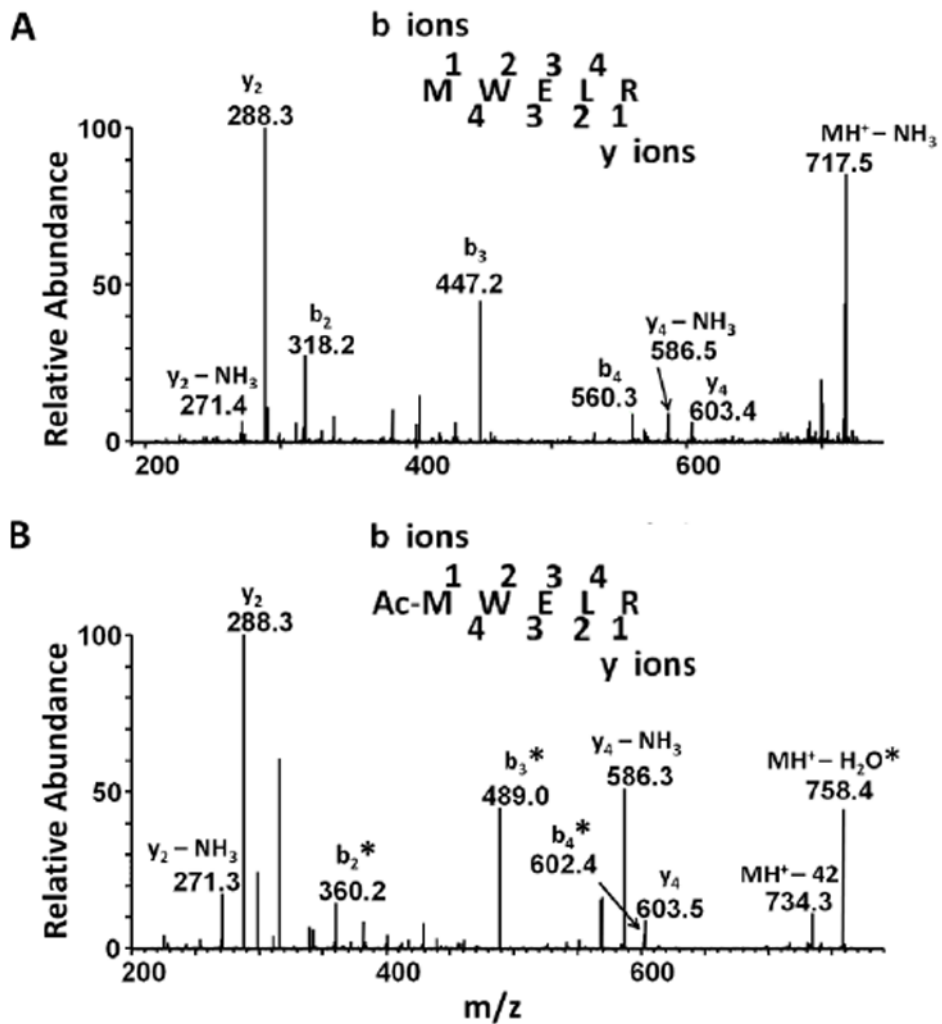


Figure 6. Identification of acetylated AQP0 1-5. MS/MS spectra from the center of a 60 year lens confirmed the identity of A) unmodified AQP0 1-5 and B) N-terminally acetylated (Ac) AQP0 1-5. Asterisks indicate acetylated b-ions. The peptide fragmentation patterns for unmodified and acetylated AQP0 are shown at the top of each panel.

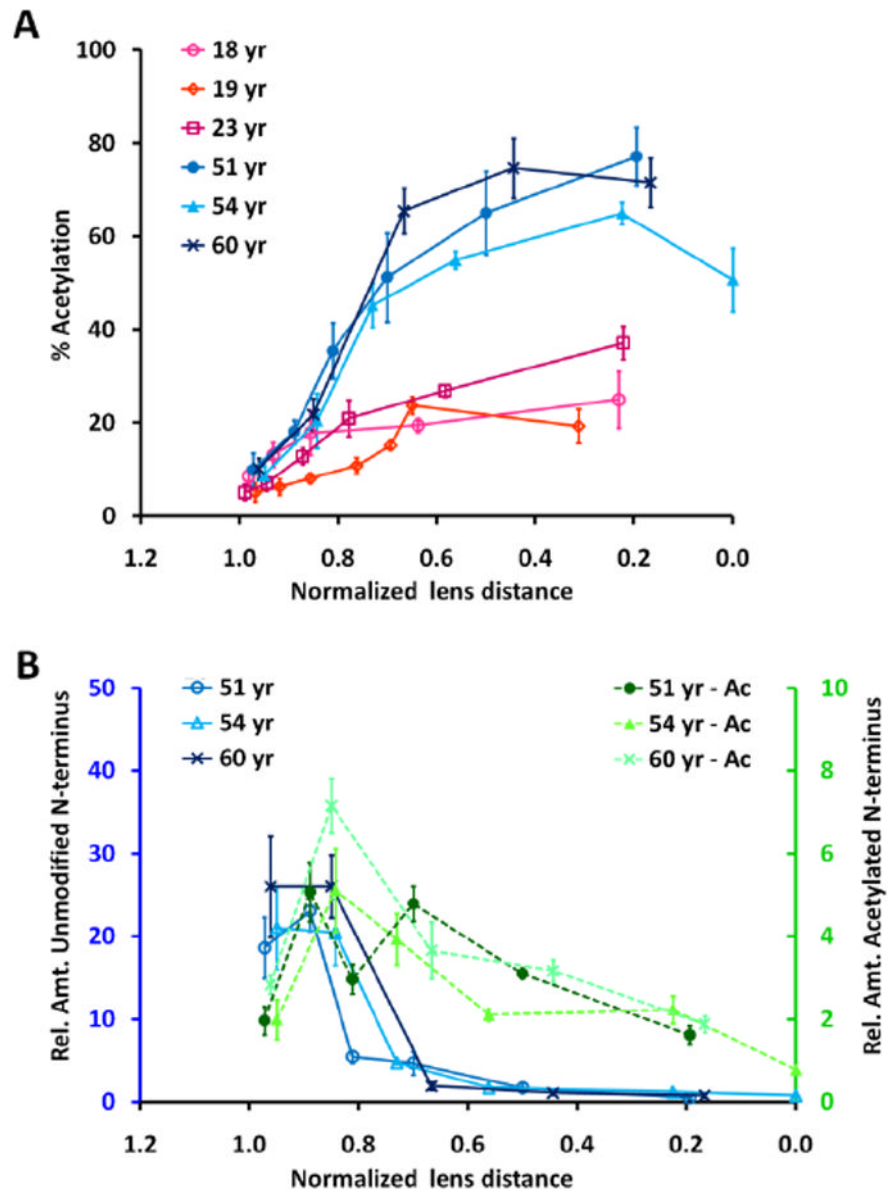


Figure 7. The distribution of acetylated AQP0 N-terminus as a function of normalized lens distance. A) The percent of AQP0 N-terminal acetylation in young and aged lenses. B) The relative amount of unmodified (left, gray axis) and acetylated (Ac, right, black axis) AQP0 N-terminus in aged lenses.

Table 1

Lens regions

Lens Regions		
Region	Normalized Lens Distance	Avg. Normalized Lens Distance
cortex	1.00-0.84	0.99 ± 0.1
AN	0.84-0.60	0.75 ± 0.1
JN	0.60 - 0.48	0.49 ± 0.1
FN	0.48 - 0.03	0.25 ± 0.03
EN	0.03 - 0.0	0.0

A description of the lens regions profiled directly from tissue. Regions are defined using developmental age and lens distance, as described by Taylor et al., (1996) – left and center columns – and by normalized lens distance, averaged over all aged lenses, as sampled in these experiments – right column. Abbreviations: AN – adult nucleus; JN – juvenile nucleus; FN – fetal nucleus; EN – embryonic nucleus.

Table 2Expected [M+H]⁺ ions of observed AQP0 products.

Expected [M+H] ⁺ of AQP0 Products			
Sequence	Unmodified [M+H] ⁺	Acetylated [M+H] ⁺	Oleoylated [M+H] ⁺
1-263	28123	28165	28387
1-259	27710	27752	27974
1-246	26359	26401	26623
1-243	26059	26101	26323